Morphometric Study of the Mare Oviductal Mucosa at Different Reproductive Stages

HORACIO MOUGUELAR,[1]* TOMÁS DÍAZ,[1] DAMIANA BORGHI,[1] ROLANDO QUINTEROS,[2] FACUNDO BONINO,[2] SILVANA ANDREA APICHELA,[3] AND JOSÉ JAVIER AGUILAR[4]

[1]Departamento de Anatomía Animal, Facultad de Agronomía y Veterinaria, Universidad Nacional de Río Cuarto, 5804 Río Cuarto, Córdoba, Argentina
[2]Departamento de Ciencias Básicas, Facultad de Agronomía y Veterinaria, Universidad Nacional de Río Cuarto, 5804 Río Cuarto, Córdoba, Argentina
[3]Instituto Superior de Investigaciones Biológicas, (CONICET), Facultad de Bioquímica, Química y Farmacia, Universidad Nacional de Tucumán, Tucumán, 4000, Argentina
[4]Departamento de Producción Animal, Facultad de Agronomía y Veterinaria, Universidad Nacional de Río Cuarto, 5804 Río Cuarto, Córdoba, Argentina

ABSTRACT

The objectives of this work were to describe some morphometric characteristics and to establish quantitative parameters of different regions of the equine oviductal mucosa from the isthmus, ampullary-isthmic junction (AIJ), and ampulla. Twenty-one mixed-bred mares were used for this study. Mares were selected in the following reproductive phases: anestrus, estrus, and diestrus. The left oviducts were examined with light microscopy, and rights ones were studied through the intraoviductal molds. The isthmus showed the smallest luminal area, mucosal area, epithelial perimeter, and luminal diameter. On the molds surfaces, some grooves extended as longitudinal canals, reducing their depth as they approached to the AIJ. Several small height projections, some obliquely positioned towards utero-tubal junction, were observed in all reproductive phases. These formations may represent pockets or cul-de-sacs in the basal areas of the epithelial folds. The AIJ mucosa gradually changed from the smooth isthmic region toward highly folded ampulla. The number and complexity of epithelial folds showed moderate increase in the same way that many of the morphometric parameters. Multiple curves were observed on the molds of the AIJ, creating a zigzag path in the oviductal lumen. In the ampulla, the high branched epithelial folds occupied most of the lumen, leaving a small luminal area free. A linear relationship between epithelial perimeter and mucosal area was found. The presence of glandular-like structures was observed in all the reproductive stages studied. The

Additional Supporting Information may be found in the online version of this article.

Grant sponsor: SeCyT- Universidad Nacional de Río Cuarto; Grant number: 18/A290.

*Correspondence to: MV. H. Mouguelar, Departamento de Anatomía Animal, Ruta 36, Km. 601, Río Cuarto, Córdoba, Argentina. Fax: +54 (0358) 4680280. E-mail: hmouguelar@ayv.unrc.edu.ar

Received 2 March 2015; Accepted 20 May 2015.
DOI 10.1002/ar.23193
Published online 30 June 2015 in Wiley Online Library (wileyonlinelibrary.com).

equine endosalpinx reveals a highly complex tridimensional arrangement where each region shows very particular and specific designs. Anat Rec, 298:1950–1959, 2015. © 2015 Wiley Periodicals, Inc.

Key words: mare; oviduct; mucosa arrangement; morphometric characteristics;reproductive stages

INTRODUCTION

The mammalian Fallopian tube plays a crucial role in many reproductive events. Gamete and embryo transport, sperm storage and final capacitation, fertilization, and early cleavage-stage embryonic development occurs in the oviductal environment (Suárez, 2008). Its specialized architecture enables this organ to coordinate these biological processes. Therefore, the reproductive success of the mammalian female depends initially on the oviduct (Hunter, 1998). In mammals, the oviduct is traditionally divided into several regions; infundibulum, ampulla, ampullary-isthmic junction (AIJ), isthmus, and uterotubal junction (UTJ) based on histological and anatomical characteristics. The gross anatomy and histology of the uterine tube has been studied in many domestic species (Barone, 1978; Banks, 1996; Bacha and Bacha, 2012). It consists of three concentric layers; the serosa (mesosalpinx) composed of mesothelial and nonstriated muscular cells derived from the uterine broad ligament; the middle muscular layer (myosalpinx) organized in a particular arrangement in different species (Muglia and Motta, 2001); and internally the mucosa (endosalpinx), with dense lymphatic and blood vascular network; adrenergic, cholinergic and peptidergic nerve fibers (Wrobel et al., 1993). The complete endosalpinx have folds that project centrally into the lumen. The height, width, and branching of the mucosa folds are more pronounced in the ampulla and the infundibular region. This inner layer is lined by a simple columnar or pseudostratified epithelium, containing ciliated and secretory cells. Ciliated cells play a role in the gamete and embryo transport (Teilmann et al., 2006; Kölle et al., 2009), in collaboration with interstitial Cajals cells present in the myosalpinx (Dixon et al., 2009). Secretory cells are mainly involved in the synthesis and release of different kinds of molecules that dissolve in the oviductal fluid, together with a selective transudate of serum (Oliphant, 1986; Willis et al., 1994; Leese et al., 2001; Hugentobler et al., 2010; Killian, 2011). Qualitative and quantitative analysis of secretory activity has been demonstrated at different oviductal regions in many mammals, eg. in the mouse (Nieder and Macon, 1987), rat (Abe and Abe, 1993), pig (Buhi et al., 1992), sheep (Buhi et al., 1991), baboon (Verhage and Fazleabas, 1988), human (Hyde and Black, 1986), goat (Gandolfi et al., 1993), and cow (Gerena and Killian, 1990). Cyclic morphometrical, ultrastructural, and histochemical changes in the oviductal epithelium have been studied in several mammalian species (Abe, 1996; Nayak and Ellington, 1997; Steinhauer et al., 2004; Abe and Hoshi, 2008; Desantis et al., 2011). These changes appear to respond to gonadal steroids concentrations across reproductive stages. Some particularities have been described about the equine oviduct, such as selective developing embryo transport (Betteridge et al., 1979; Weber et al., 1991), luminal collagen-cellular masses (Aguilar et al., 1997; Lantz et al., 1998), trabeculae of connective tissue dividing the lumen (Aguilar et al., 2012), and crypts or glandular-like structures in the mucosa (Aguilar et al., 2010). Other reports have been published in relation to lymphocyte subset characterization (Brinsko and Ball, 2006), *in vitro* sperm–epithelium interaction (Ellington et al., 1993; Thomas et al., 1994), isolation of μ-opiod receptors (Desantis et al., 2008), and localization of glycoconjugates in the epithelium (Desantis et al., 2004, 2005). Recently, prostaglandin E2 receptors have been characterized (Ball et al., 2013) and steroids regulation of gene expression (Nelis et al., 2012). Aguilar et al. (2012) described some histological characteristic in the mare oviductal epithelium at different reproductive stages. However, many morphometric features of the luminal surface and tridimensional conformation of the mucosa in the mare oviduct have not been described yet. Therefore, the primary aim of this study was to describe some morphometrical characteristics of the endosalpinx in transverse histologic oviductal sections. In addition, other quantitative parameters from isthmus, AIJ, and ampullary region at different reproductive phases were studied through intraoviductal corrosion casts.

MATERIALS AND METHODS

Animals

Twenty-one nonpregnant mixed-bred mares, 3–14 years old, were selected at a slaughterhouse located 5 km from our laboratory. Reproductive stages were determined by rectal palpation and ultrasonography of the genital tract. Animals were selected in each of the following phases: anestrous mares (N = 6) with small ovaries, follicles <15 mm, and without corpus luteum; estrous mares (N = 9) with at least one follicle >35 mm, uterine edema, and low uterine tone; and diestrous mares (N = 6) with an ultrasonographically visible corpus luteum, increased uterine tone, and no uterine edema. Anestrous and estrous mares were assigned to be slaughtered on the day of selection, whereas diestrous mares were monitored until ovulation and then assigned to be slaughtered on days 7 or 8 after ovulation.

Sampling

Genital tracts were collected immediately after slaughter and transported to the laboratory within 1 hr in 37°C tempered saline solution. Reproductive phases were confirmed through ovarian structures examination. Dissection was carried out to isolate the oviduct from the rest of the reproductive tract. After dissection, the

left oviduct was reserved for light microscopy (anestrus N = 6, estrus N = 9, diestrus N = 6) and the right one for intraluminal corrosion casts (anestrus N = 5, estrus N = 5, and diestrus N = 4). Seven oviducts were damaged during the dissection procedure and therefore discarded.

Light Microscopy Examination

For histology, portions measuring 1 cm were taken from the isthmus 2 cm proximal to the uterine-tubal junction, the AIJ at about the middle third of the oviduct and the ampulla at a distance of 2 cm distal from the fimbria. Oviductal segments were fixed overnight in BFS solution (pH 7,4), washed and dehydrated in ethanol series, cleared in xylene, and embedded in paraffin wax. Transverse tissue sections 7 μm thick were cut, and after dewaxing with xylene and hydration in an ethanol series of descending concentrations they were stained with hematoxylin and eosin. Morphological characteristics from oviductal sections were examined using digital stereomicroscopy[1]. Photomicrographs were taken at 40× magnification and, morphometric quantifications were registered using the software tools[2]. To measure all variables, tissue sections obtained were analyzed only transversely. The following parameters were measured: luminal area (LA), epithelial perimeter (EP), and mucosal area (MA). Mucosal area was calculated from the difference between cross sectional area (CSA) and luminal area. CSA was obtained measuring major and minor diameter to transverse sections (including epithelium and muscular layer but not serosa) and using the formula $(A = \pi \times D^2/4)$. Approximate volume (μL) was calculated from the multiplication of the LA and length of each tubular oviductal region.

Intraoviductal Corrosion Cast and Morphometric Evaluation

Fourteen oviducts at different reproductive stages were used to create intraluminal casts using a low viscosity polyurethane resin[3]. This resin was originally created for building casts accurately from cadaveric small blood vessels (capillaries) and quantitative analysis by scanning electron microscopy. For intraoviductal injection, the resin was stained with pigment powder (at 1–2%, v/v)[4], previously dissolved in methyl-ethyl-ketona (at 30%, v/v)[5]. Shortly before the injection, the hardener[6] (ratio 100:16 v/v) was added. The utero-tubal junction (UTJ) was dissected and the oviductal papilla channeled with a 25G needle. To create resin molds from the UTJ, retrograde injection was performed (from isthmic region to uterine horn, cranial tip). The oviduct was kept 24 for hours in saline tempered solution, until complete resin polymerization. The samples with surrounding and support tissues were immersed overnight in corrosion solution (KOH 7.5% at 50°C). After the corrosion process, the intraluminal casts were washed in distilled water and air-dried (Fig. 1, Supporting Information). Molds obtained were observed and photomicrographed using Motic Images Plus 2.0^{ML} digital stereomicroscopy to obtain morphometrical parameters. According to the macroscopic characteristics, each region (isthmus, AIJ, and ampulla) was sequentially photographed along its length. Of each mold, 15 images of the isthmus were taken, 5 of the AIJ, and 10 of the ampulla. Each image included a segment of 6.4 mm length to the segment evaluated, and five equidistant transverse measures were made to determined segment luminal diameter (LD, μm). Values obtained from central segment were taken as representative of each region. One additional measure along median axis to determine segment length (mm) was taken (Fig. 2, Supporting Information).

In addition, some molds were analyzed by scanning electron microscopy (SEM). They were mounted on aluminium stubs, coated with gold, and examined in a Carl Zeiss® Supra 55VP scanning electron microscope (USA).

Statistical Analysis

Data were analyzed to assess the effect of the reproductive stages of the estrous cycle (anestrus, estrus, and diestrus) on the fallopian tube region (isthmus, AIJ, and ampulla) on LA, EP, MA, LD, and SL. Variables were assessed for normality using the Shapiro-Wilks modified test and analyzed using ANOVA and Tukey's post hoc test.

RESULTS

Intraluminal molds from all processed oviducts revealed an internal tortuous pathway in the different regions of the duct, being very pronounced in the AIJ. On the molds surface, the oviductal mucosa left many grooves with different directions and depths marked, according to the number and branching to the epithelial folds, whose height, category, and branches increased from the isthmus to ampulla.

Isthmus

In all histological sections, a narrow luminal area not exceeding 0.5 mm^2 was found (Table 1), with no significant differences between reproductive stages ($P > 0.05$). In photomicrographs, eight to ten broaden-base and rounded primary folds, separated by shallow grooves radially organized were observed (Fig. 3A). These few primary folds and their low height determined an epithelial perimeter of few millimeters.

Histological sections with large mucosal area, showed a linear increase in the epithelial perimeter ($r^2 = 0.78$). However, in this segment, the lowest perimeter compared to the other tubular regions was found, without significant differences between reproductive stages (Table 1).

As in the histological sections, three-dimensional resin molds showed that caudal isthmus and UTJ (papilla, not shown) had the lowest luminal diameter, with no significant differences among reproductive stages evaluated ($P > 0.05$, Table 1). On the molds surfaces, three or four grooves (corresponding to primary folds) extended as a continuous longitudinal canal, reducing their depth as they approached the AIJ (Fig. 3B–D). Several low height projections, arranged in rows and

[1]Motic DM 39C-N9GO.

[2]Motic Images Plus 2.0^{ML}, China Group Co., Ltd.

[3]PU4ii® *polyurethane for improved imaging;* vasQtec; Zurich–Switzerland.

[4]Farbpaste DW- 0113-5®

[5]MEK, Taurus®, Argentina.

[6]PU4ii Hardener®; vasQtec; Zurich, Switzerland.

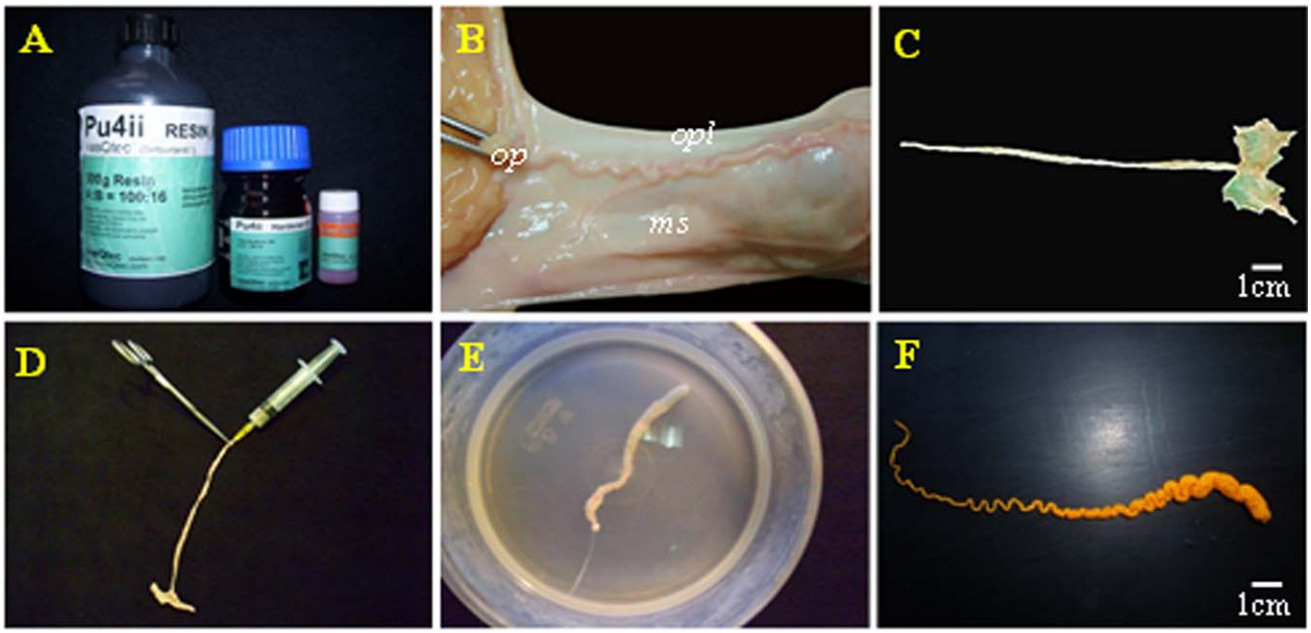

Fig. 1. Technique for intraoviductal repletion cast. **A**: PU4ii®, hardener and pigment; **B**: papilla (op) and the isthmus of the oviduct with the mesosalpinx (ms) and ovarian proper ligament (opl); **C**: dissected and displayed oviduct; **D**: channeled papilla and fixation of the needle by Halsted forceps; **E**: immersed in corrosive solution; F: mold of oviductal lumen (without infundibulum) after complete corrosion of tissue.

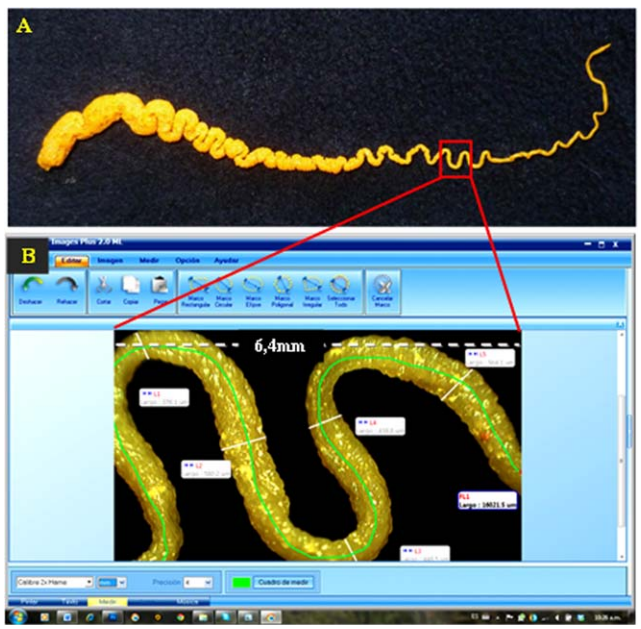

Fig. 2. **A**: Resin mold of the oviduct (without infundibulum) where a segment is highlighted in the cranial isthmus; **B**: segment (6.4 mm long) of the cranial isthmus, registered with Motic DM 39C-N9GO digital stereomicroscope at 40×. Image analysis with the Motic Images Plus 2.0ML software: white lines in five measurements are to determine the width; and the green line marked on the median axis to measure the length.

separated by small-interconnected secondary grooves, some obliquely positioned toward utero-tubal junction, were observed in all phases of the estrous cycle (Fig. 3D). These formations may represent crypts, pockets, or cul-de-sacs in the isthmic mucosa.

The caudal isthmus lumen, near the UTJ, was arranged more rectilinearly and in the remaining segment, sigmoid shaped curves were observed, becoming more U or V-shaped toward the AIJ (Fig. 2A, Supporting Information and Fig. 3C). Isthmic region was the longest segment of the oviduct, and with no significant differences between reproductive stages ($P > 0.05$, Table 2).

Ampullary-Isthmic Junction

The luminal area and epithelial perimeter determined from histological sections increased substantially in the AIJ compared with the isthmic region, showing significant differences between reproductive stages ($P < 0.05$, Table 1). The number and branching of epithelial folds showed also considerably increase in the AIJ versus the isthmus. Tertiary and sometimes quaternary folds were observed in the junction and in the caudal ampulla. In basal areas of the primary folds, epithelial crypts were observed (Fig. 4A). In the AIJ as well as in the isthmus, a linear relationship between epithelial perimeter and mucosal area was found ($r^2 = 0.80$).

The morphology of the AIJ endosalpinx gradually changed from the isthmus toward the ampullary region. This finding was also observed on the surface of the resin molds. The three-dimensional luminal casts showed a moderate complexity in their folds and grooves compared with the smooth isthmus and high-folded ampulla. Most primary folds branched and divided longitudinally with a perpendicular or oblique position, creating a pattern of folds and grooves without a clear and definite order on molds surfaces (Fig. 4C,D). This region showed a slight increase in the luminal diameter, from

TABLE 1. Oviduct Morphometric Parameters at Different Reproductive Stages

Stage	Isthmus				Ampullary-isthmic junction				Ampulla			
	LA (mm^2)	EP (mm)	MA (mm^2)	LD (mm)	LA (mm^2)	EP (mm)	MA (mm^2)	LD (mm)	LA (mm^2)	EP (mm)	MA (mm^2)	LD (mm)
Anestrus	0.21	4.15	0.42	499.64	2.19	48.79	3.47	1850.09	2.10	80.58	6.46	3902.52
	(0.11)	(1.64)	(0.24)	(4.87)	$(0.92)^{ab}$	$(15.52)^{a}$	$(1.28)^{ab}$	$(55.09)^{a}$	(0.35)	(29.87)	(1.93)	$(916.20)^{a}$
Estrus	0.25	3.61	0.36	491.87	1.07	17.80	1.52	1716.07	2.43	51.83	5.71	3737.93
	(0.09)	(1.82)	(0.15)	(7.97)	$(0.69)^{a}$	$(14.92)^{b}$	$(1.19)^{a}$	$(63.79)^{a}$	(1.51)	(26.49)	(2.85)	$(984.44)^{a}$
Diestrus	0.24	3.75	0.41	500.83	2.51	45.50	4.80	2549.34	2.72	89.48	6.81	4903.94
	(0.19)	(1.47)	(0.30)	(7.04)	$(1.35)^{b}$	$(5.43)^{a}$	$(1.41)^{b}$	$(78.99)^{b}$	(0.73)	(25.49)	(1.63)	$(933.95)^{b}$
P value					<0.01	<0.001	<0.002	<0.001				<0.001

Abbreviations: LA, luminal area; EP, epithelial perimeter; MA, mucosal area; LD, luminal diameter; AIJ, ampullary-isthmic junction.
Different superscripts indicate statistical differences ($P < 0.05$).
Results are mean (± S. E).

Fig. 3. **A**: Histological section of the central portion of the isthmic region (H & E stained), showing broaden-base primary folds and radially arrangement grooves, and some lateral cul-de-sacs in basal areas (arrows); **B**: cross-sectional of luminal cast of the isthmus, where eight to ten grooves and folds were observed with digital stereomicroscope at 40×; **C**: Scanning electron microscopy (SEM, 45×) of the resin mold of the isthmus, showing grooves like longitudinal channels along it (arrows); **D**: low height projections (molds of the cul-de-sacs), arranged in rows (arrowheads) and separated by small-interconnected secondary grooves, some obliquely positioned toward utero-tubal junction, SEM, 125×. Some small air bubbles were located in depth of primary and secondary grooves. Scale bar in A and B indicates 250 μm and in C and D, 200 μm.

its junction with the isthmus, toward the ampulla, with some differences among the reproductive stages studied (Table 1).

Multiple continuous W-shaped curves were observed on the molds of this region (Fig. 4B). They were produced by transverse folds of subserous connective tissue that penetrated from opposite sides (mesosalpinx and antimesosalpinx), creating a sinuous and zigzag path in the oviductal lumen.

Ampulla

In histological sections and in all reproductive stages, multiple epithelial folds of different complexity were found; frequently short quaternary folds were also

TABLE 2. Length (mm) of the Different Regions of the Oviduct at Different Reproductive Stages, Calculated from Resin Molds

Region	Anestrus (N = 6)	Estrus (N = 9)	Diestrus (N = 6)	*P* value	Length in all stages
Isthmus	96.36 (4.31)	108.02 (7.14)	88.71 (6.39)	>.05	96.78 (3.32)[a]
AIJ	48.03 (3.63)	45.89 (6.02)	58.57 (5.38)	>.05	50.24 (3.62)[b]
Ampulla	89.44 (4.86)	89.71 (8.06)	74.12 (7.21)	>.05	85.66 (4,34)[a]
TLO	205.53 (9.99)	236.32 (16.57)	194.21 (14.82)	>.05	
P value					<0.001

Different superscripts indicate statistical differences among regions of oviduct ($P < 0.05$).
Abbreviations: AIJ, ampullary-isthmic junction;TLO, total length of the oviducts.
Results are mean (± S. E).

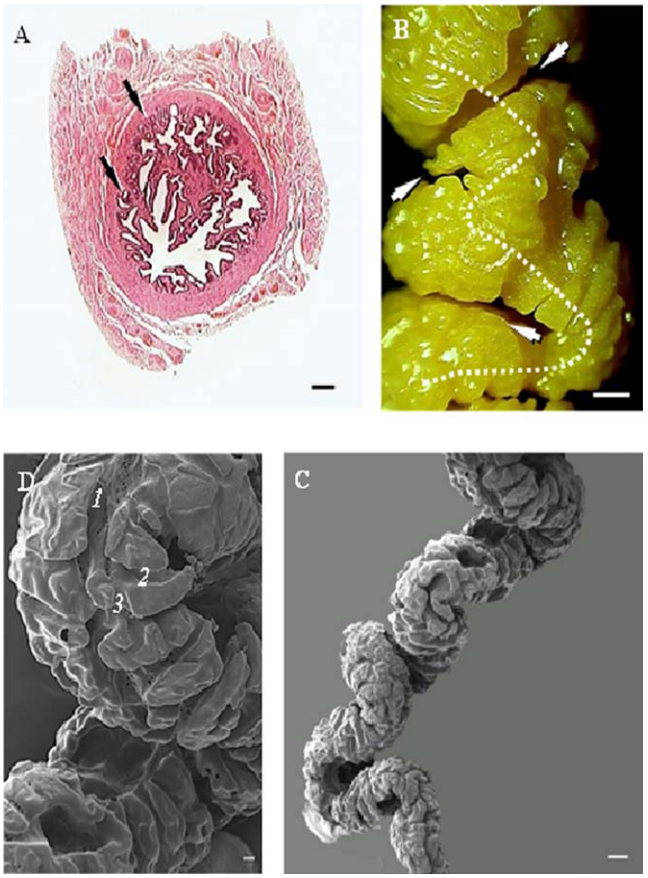

Fig. 4. **A**: Histological cross-section of the central portion of the ampullary-isthmic junction (AIJ), with hematoxylin and eosin stain, showing different categories of epithelial folds and some crypts (glandular-like structures) in basal areas (arrows); **B**: stereomicroscopy of resin mold of the AIJ, where deep and opposite grooves (arrows) produce W-shape curves (dotted line) and sinuous path in the lumen (40x); **C**: Scanning electron microscopy (SEM, 21x) of the resin mold of the AIJ showing a tortuous path and complex system of folds and grooves without specific organization; **D**: primary (1), secondary (2) and tertiary (3) shallow grooves, produced by epithelial folds, SEM, 70×. Scale bar in A and D, indicates 100 μm, in B 500 μm, and in C 1mm.

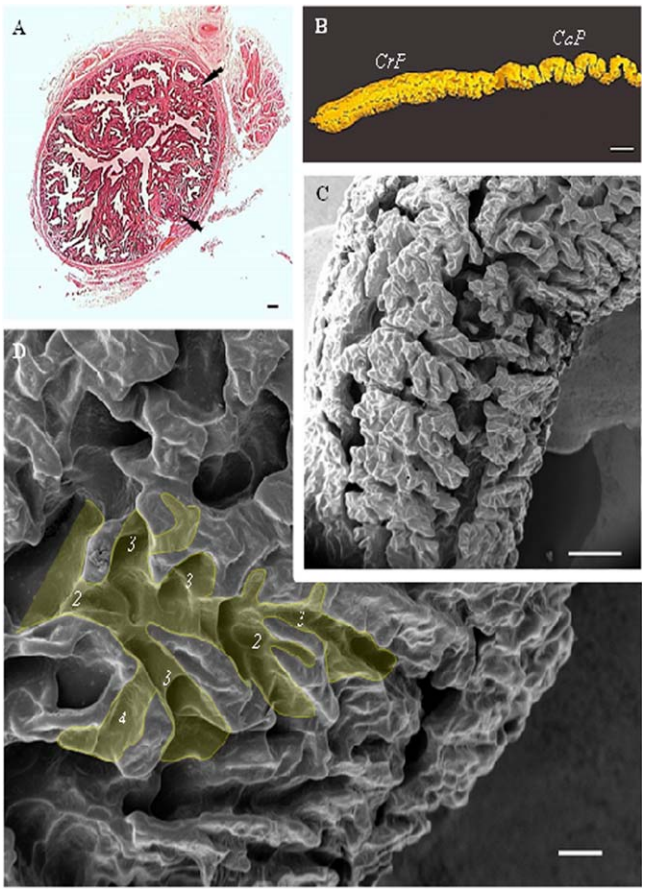

Fig. 5. **A**: Photomicrograph of the central portion of the ampulla, (H & E), where primary, secondary, tertiary, and quaternary folds occupied most of its lumen. Numerous epithelial crypts (glandular-like structures) in folds are shown (arrows); **B**: low magnification stereomicroscopy (7.5×) of the mold of the ampulla, showing some curves in the caudal portion (CaP), that gradually disappear toward its cranial portion (CrP), where the lumen of ampulla becomes a rectilinear path; **C**: Scanning electron microscopy (SEM, 33×) of the resin mold of the ampulla showing the intricate arrangement of the ampullary endosalpinx; **D**: branching of the primary, secondary (2), tertiary (3), and quaternary (4) grooves (highlighted), corresponding to different categories of epithelial folds, SEM, 65×. Scale bar in A indicates 100 μm, in B 5 mm, in C 1 mm, and in D 200 μm.

observed (Fig. 5A). Primary, secondary, tertiary, and quaternary folds occupied most of the lumen, leaving a small luminal area free. No significant differences among the reproductive stages were detected ($P > 0.05$, Table 1). Such as in AIJ, numerous epithelial crypts (glandular-like structures) in basal areas of primary folds were found (Fig. 5A).

TABLE 3. Approximate Volume (μL) of the Different Regions of the Oviduct Among Reproductive Stages, Calculated from Histological Section

Stage	Isthmus	AIJ	Ampulla
Anestrus	21.54 (9.09)	125.05 (36.93)[a]	504.46 (38.73)[a]
Estrus	37.16 (5.03)	46.08 (18.03)[b]	283.63 (53.63)[ab]
Diestrus	21.84 (7.04)	108.02 (7.14)[a]	203.92 (51.90)[b]
P value	>.05	<0.005	<0.01

Different superscripts indicate statistical differences among regions of oviduct ($P < 0.05$).
AIJ, ampullary-isthmic junction.
Results are mean (±S. E).

In resin molds, irregular grooves of different depth, width, and orientations were observed, showing the intricate arrangement of the ampullary endosalpinx. Some longitudinal, deep and asymmetrical grooves (corresponding to the primary folds) were oriented toward infundibular region, separating or joining with other multiple small and shallow lateral grooves (Fig. 5C,D).

The numerous and branched epithelial folds induced a substantial increase in epithelial perimeter, compared with isthmic and ampullary-isthmic region. This finding was observed in all reproductive stages of the estrous cycle (Table 1). Similarly to the AIJ and isthmus, in this ampullary region, a linear relationship between epithelial perimeter and mucosal area was found ($r^2 = 0.79$).

In the molds, the caudal portion of the ampulla (near to AIJ) showed several curves in the lumen, gradually disappearing into the cranial portion and toward the infundibulum, where the lumen of ampulla adopted a rectilinear path (Fig. 5B).

In this tubular segment of the oviduct, a larger intraluminal diameter was found, and some significant differences between the reproductive stages evaluated were observed (Table 1).

The difference in the total length of the oviducts at different reproductive stages was not statistically significative (Table 2). The approximate volume in microliters (μL) showed differences for each tubular region and some phases of the estrous cycle (Table 3).

DISCUSSION

The gross anatomy of the oviduct of numerous species of domestic mammals has been extensively documented (Barone, 1978). Such as in the pig, cow, sheep, goat and other mammals, the mare oviduct presents different curves or convolutions, whose shape varies at different morphological regions of the fallopian tube. Duct tortuosity is closely related to the oviduct length (Hunter, 1988), such as in the female rabbit, which has short and practically straight oviducts (Pedrero-Badillo et al., 2013). In sows, the length (and degree of sinuosity) increases after first estrus post-weaning (Rigby, 1968), and in cows the fallopian tubes growth is completed after puberty (Hunter, 1988). In the mare, this information has not been documented yet.

Several anatomical descriptions determined that the oviduct of the mare is the longest of all species of domestic mammals, reaching an average of 20 cm (Getty, 1982; Dyce et al., 2010), and often 30 cm in length (Barone, 1978). One report describes some morphometric details through direct observation of dissected mare's oviducts (Suzuki and Tsutsumi, 1979). They found a length of 20.9 ± 1.2 cm from the oviducts evaluated. In the present study, from the intraluminal molds, and in agreement with the previous literature, similar lengths were found. However, in this work the infundibular region was not included, which would add a few centimeters more to the whole length of the fallopian tubes in the mare.

Of the different tubular regions of the duct, the isthmus had numerous curves along its path in all reproductive stages evaluated. This finding probably made the isthmic region the longest of all the regions of the tube evaluated. In agreement with Suzuki and Tsutsumi (1979) and Dyce et al. (2010), the length of the isthmus showed no statistical differences with the ampullary region. Despite the large number of curves found, the length of AIJ was approximately 2.5 times shorter than the isthmic and ampullary region of the oviduct.

The curves on the AIJ (produced by transverse folds of subserous connective tissue) and the sinuous path observed in the oviductal molds are consistent with previous histological findings (Aguilar et al., 2012).

The lengths at the different regions of the oviduct, in relation to hormonal milieu or at different reproductive stages, have received little attention. Lewis and Berardinelli (2001) described some gross morphometric and histomorphometic changes in oviducts of post-pubertal transition and mature ewes. The length of the isthmus and ampulla from mature ewes was longer than those for postpubertal transition sheep. In the present study, no significant differences for this morphometric measure between reproductive stages were observed.

The internal morphometry of the different tubular regions of the oviduct have been studied in rabbit (Leese, 1983; Pedrero-Badillo et al, 2013), bovine (Yániz et al., 2000), swine (Suárez, 2008), ovine (Yániz et al., 2013), and canine (England et al., 2013) oviducts. These previous studies described the internal diameter, the luminal area, luminal perimeter, and area of folds protruding into the oviduct lumen. In agreement with these studies, we found that the isthmus of the mare oviduct had the most constricted lumen of all portions of the duct. The present study shows that the isthmus presented a luminal diameter around to 300 microns near to the utero-tubal junction (oviductal papilla, data not shown), around 500 microns in its middle part, and approximately one millimeter (1 mm) at the join with the AIJ.

Although in our study no differences were found in the luminal diameter of the isthmus among reproductive stages, the mucosal edema, muscle contraction, and vascular congestion have been observed in the isthmic region in the sow (Hunter, 1973, 1975a, 1975b, 2012) and cow (Suárez, 2002) oviduct, during estrus and periovulatory stage. This could explain the decrease in luminal diameter at this reproductive stage in their studies.

According to Suzuki and Tsutsumi (1979), the external and internal diameter (lumen) of the oviduct gradually increased from isthmus toward the ampulla. Similarly, in our study the middle part of the ampulla had the largest diameter (4–5 millimeters approximately) among reproductive stages.

The equine endosalpinx presents epithelial folds with different degree of branching and morphology, showing the ampullary region a higher degree of complexity

(Trautman and Fiebiger, 1952; Barone, 1978; Bacha and Bacha, 2012). Our results showed that the number and branching of epithelial folds increased significantly from the isthmus to the ampulla, where tertiary and quaternary folds were found frequently in all histological sections and reproductive stages. This finding was not observed in the same way in the three-dimensional molds because the epithelial folds were partially flattened during filling of the lumen with the resin. The luminal perimeter showed significant changes between regions of the equine fallopian tube. The low-folded isthmic mucosa produced the lowest luminal perimeter compared to the AIJ and highly folded ampullary region. The larger luminal perimeter of the ampullary region provides a large contact surface to support biological events such as embryo development. Possibly this is related to the fact that the ampulla appears to be the most active secretory region, where more fluid is produced by epithelial cells, supplying the necessary nutrients for gamete meeting, fertilization, and early cleavage of embryos. Leese (1983) found similar results in rabbit oviduct, where more fluid was produced in the ampulla than in the isthmic region, reflecting the greater surface area of the first one.

Ampullary-isthmic junction during estrus had the smallest luminal perimeter and diameter compared with the samples obtained in anestrus and diestrus. This finding may be because of edema, thickening of the folds and hypertrophy or hyperplasia of epithelial cells in response to circulating estrogens. England et al., (2013) found similar results along the length of the bitch uterine tube at different stages of the estrous cycle. Although the isthmus has a smaller epithelial surface outline (perimeter) for sperm binding, studies on pig (Suárez et al., 1991), equine (Thomas et al., 1994), human (Baillie et al., 1997), rat (Orihuela et al., 1999), and cow (Suárez et al., 1997; Sostaric et al., 2008) have shown that spermatozoa preferentially bind to the isthmic mucosa *(in vitro* and *in vivo)* compared with the ampulla. In the same study, England et al., (2013) observed some differences in epithelial surface outline (perimeter) among reproductive stages. In the metoestrus and diestrus they found the smallest perimeter compared with proestrus and estrus in all regions of the bitch oviduct.

It could be suggested that some folds and grooves may be continuous along the isthmus, AIJ, and ampulla. Through the molds, it was possible to replicate with enough detail the complex tridimensional architecture of the endosalpinx of the ampulla, with folds of different height, category and tridimensional arrangement.

There is consensus in relation to the absence of glands in the oviduct of most domestic mammals (Banks, 1996; Bacha and Bacha, 2012). However, in all histological sections and at different reproductive stages, epithelial crypts, whose organization resembles glandular structures were found, reinforcing previous histological descriptions (Aguilar et al., 2010). In agreement with reports for other species, such as rabbits (Jansen and Bajpai, 1982), cows (Yániz et al., 2000), cats (Chatdarong et al., 2004), bitches (Steinhauer et al., 2004), sows (Ekhlasi-Hundrieser et al., 2005; Tummaruk and Tienthai, 2010), and sheep (Yániz et al., 2013) these crypts were observed in the equine oviductal mucosa in histological sections and some molds like small projections.

There are few morphological studies of the mare oviductal mucosa by scanning electron microscopy. The existence of different subcompartments, cul-de-sacs and crypts in the mucosa is widely described in the oviduct of the sow (Wu et al., 1976; Yániz et al., 2006), cow (Yániz et al., 2000), and recently in the sheep (Yániz et al., 2013). Our findings from histology and tridimensional molds suggests that the equine endosalpinx is arranged in a very complex way and has all these different subcompartments, sacculations, or cul-de-sacs at different regions, suggesting that each segment has particular functions.

Since the 1990s oocyte transfer has been used to obtain pregnancies from mares considered infertile using standard breeding methods or embryo transfer (Carnevale et al., 2005). In these technologies, empirical volumes of 0.1 to 0.3 milliliters of transfer medium deposited into the cranial ampulla were used during oocyte transfer (OT) (Hinrichs et al., 1998; Carnevale et al., 2001). In this study, we found an approximate volume of ~215–345 μL for the ampulla that can house the volumes used in OT during estrus stage. The values found in the present study partially agree with those reported for the oocyte transfer technic.

CONCLUSIONS

The combination of histology and intraluminal molds allowed us to characterize some morphometric parameters of oviductal lumen of the mare at different reproductive stages. The findings presented provide useful information to build a more complete model on the three-dimensional organization of the oviductal mucosa of the mare. Knowing the anatomic, histologic, and physiologic complexity of this organ may be relevant for improving the application of assisted reproductive technologies in horses.

ACKNOWLEDGEMENT

All authors have made substantial contributions to the research design and to the collection, analysis, and interpretation of data. Dr. Javier Aguilar acts as head of the research group.

LITERATURE CITED

Abe H. 1996. The mammalian oviductal epithelium: regional variations in cytological and functional aspects of the oviductal secretory cells. Histol Histopathol 11:743–768.

Abe H, Abe M. 1993. Immunological detection of an oviductal glycoprotein in the rat. J Exp Zool 266:328–335.

Abe H, Hoshi H. 2008. Morphometric and ultrastructural changes in ciliated cells of the oviductal epithelium in prolific Chinese Meishan and large white pigs during the oestrous cycle. Reprod Dom Anim 43:66–73.

Aguilar JJ, Woods GL, Miragaya MH, Olsen LM. 1997. Living fibroblast cells in the oviductal masses of mares. Equine Vet J 25(Suppl): 103–108

Aguilar JJ, Cuervo-Arango J, Mas C, Reyley M, Rodriguez MB, Mouguelar H. 2010. Glands in the oviductal mucosa of the mare. Reprod Fert Dev 22:226.

Aguilar JJ, Cuervo-Arango J, Mouguelar H, Losinno L. 2012. Histological characteristics of the equine oviductal mucosa at different reproductive stages. J Equine Vet Sci 32:99–105.

Bacha WJ and Bacha LM. 2012. Female reproductive system. In: Color atlas of veterinary histology. 3rd ed. Wiley-Blackwell, Iowa. p 243–265.

Baillie HS, Pacey AA, Warren MA, Scudamore IW, Barratt CLR. 1997. Greater numbers of human spermatozoa associate with

endosalpingeal cells derived from the isthmus compared with those from the ampulla. Hum Reprod 12:1985–1992.
Ball BA, Scoggin KE, Troedsson MHT, Squires EL. 2013. Characterization of prostaglandin E receptors (EP2, EP4) in the horse oviduct. Anim Reprod Sci 142:35–41.
Banks WJ. 1996. Epitelios. En: Histología Veterinaria Aplicada. Ed. El Manual Moderno, S. A. de C. V. México-Santa Fe de Bogotá. p 79–92.
Barone R. 1978. Appareil Uro-genital. En: Anatomie comparée des Mammifères Domestiques. Imprimeri Des Meaux-Arts, J.Tixier & Fils. S.A, Lyon, France. p 311–321.
Betteridge KL, Eaglesome MD, Flood PF. 1979. Embryo transport through the mare's oviduct depends on cleavage and is independent of the ipsilateral corpus luteum. J Reprod Fertil Suppl 27: 387–394.
Brinsko SP, Ball BA. 2006. Characterization of lymphocyte subsets in the equine oviduct. Equine Vet J 38:214–218.
Buhi WC, Ashworth CJ, Bazer FW, Alvarez IM. 1992. In vitro synthesis of oviductal secretory proteins by estrogen-treated ovariectomized gilts. J Exp Zool 262:426–435.
Buhi WC, Bazer FW, Alvarez IM, Mirando MA. 1991. In vitro synthesis of oviductal proteins associated with estrus and 17β-estradiol treatment of ovariectomized ewes. Endocrinology 128: 3086–3095.
Carnevale EM, Coutinho da Silva MA, Panzani D, Stokes JE, Squires EL. 2005. Factors affecting the success of oocyte transfer in a clinical program for subfertile mares. Theriogenology 64:519–527.
Carnevale EM, Squires EL, Maclellan LJ, Alvarenga MA, Scott TJ. 2001. Use of oocyte transfer in a commercial breeding program for mares with reproductive abnormalities. J Am Vet Med Assoc 218:87–91.
Chatdarong K, Lohachit C, Linde-Forsberg C. 2004. Distribution of spermatozoa in the female reproductive tract of domestic cat in relation to ovulation induced by natural mating. Theriogenology 62:1027–1041.
Desantis S, Acone F, Corriero A, Deflorio M, Suban D, Ventriglia G, Palmieri G, De Metrio G. 2004. Distribution of sialoglycoconjugates in the oviductal isthmus of the horse during anoestrus, oestrus and pregnancy: a lectin histochemistry study. Eur J Histochem 48:403–412.
Desantis S, Albrizio M, Ventriglia G, Deflorio M, Guaricci AC, Minoia R, De Metrio G. 2008. The presence of the mu-opioid receptor in the isthmus of mare oviduct. Histol Histopathol 23: 555–564.
Desantis S, Ventriglia G, Suban D, Corriero A, Deflorio M, Acone F, Palmieri G, Metrio DG. 2005. Differential lectin binding patterns in the oviductal ampulla of the horse during oestrus. Eur J Histochem 49:33–44.
Desantis S, Zizza G, Accogli F, Acone R, Rossi R, Resta L. 2011. Morphometric and ultrastructural features of the mare oviduct epithelium during oestrus. Theriogenol 75:671–678.
Dixon RE, Hwang SJ, Henning GW, Ramsey KH, Schripsema JH, Sanders KM, Ward SM. 2009. Chlamydia infection causes loss of pacemaker cells and inhibits oocyte transport in the mouse oviduct. Biol Reprod 80:665–673.
Dyce KM, Sack WO, Wensing CJG. 2010. The pelvis and reproductive organs of the horse. In: Textbook of veterinary anatomy. 4th ed. Saunders-Elsevier, Atlanta. p 568–578.
Ekhlasi-Hundrieser M, Gohr K, Wagner A, Tsolova M, Petrunkina A, Töpfer-Petersen E. 2005. Spermadhesin AQN1 is a candidate receptor molecule involved in the formation of the oviductal sperm reservoir in the pig. Biol Reprod 73:536–545.
Ellington JE, Ball BA, Yang X. 1993. Binding of stallion spermatozoa to the equine zona pellucida after coculture with oviductal epithelial cells. J Reprod Fertil 98:203–208.
England GCW, Burgess CM, Clutterbuck AL, Freeman SL. 2013. Epithelial surface changes and spermatozoa storage in the reproductive tract of the bitch. Vet J 195:185–191.
Gandolfi F, Passoni L, Modina S, Brevini TAL, Varga Z, Lauria A. 1993. Similarity of an oviduct-specific glycoprotein between different species. Reprod Fertil Dev 5:433–443.
Gerena RL, Killian GJ. 1990. Electrophoretic characterization of proteins in oviduct fluid of cows during the estrous cycle. J Exp Zool 256:113–120.
Getty R. Sistema Urogenital de los equinos En: Sisson S y Grossman JD, Anatomía de los animales domésticos, Elsevier-Masson, 5ta. Ed. 1982, p 605–614.
Hinrichs K, Matthews GL, Freeman DA, Torello EM. 1998. Oocyte transfer in mares. J Am Vet Med Assoc 212:982–986.
Hugentobler SA, Sreenan J, Humpherson P, Leese H, Diskin M, Morris D. 2010. Effects of changes in the concentration of systemic progesterone on ions, amino acids and energy substrates in cattle oviduct and uterine fluid and blood. Reprod Fertil Dev 22: 684–694.
Hunter RHF. 1973. Transport, migration, and survival of spermatozoa in the female genital tract: species with intrauterine deposition of semen. In: ESE Hafez & C Thibault, editors. Sperm Transport, Survival and Fertilizing Ability. INSERM, Paris. pp. 309–342.
Hunter RHF. 1975a. Physiological aspects of sperm transport in the domestic pig, *Sus scrofa*. I. Semen deposition and cell transport. Br Vet J 131:565–573.
Hunter RHF. 1975b. Physiological aspects of sperm transport in the domestic pig, *Sus scrofa*. II. Regulation, survival and fate of cells. Br Vet J 131:681–690.
Hunter RHF. 1988. The fallopian tubes. "Their role in fertility and infertility". Springer-Verlarg: Berlin, Heidelberg.
Hunter RHF. 1998. Have the fallopian tubes a vital role in promoting fertility? Acta Obstet Gynecol Scand 77:475–486.
Hunter RHF. 2012. Components of oviduct physiology in eutherian mammals. Biol Rev 87:244–255.
Hyde BA, Black DL. 1986. Synthesis and secretion of sulphated glycoproteins by rabbit oviduct explants in vitro. J Reprod Fertil 78: 83–91.
Jansen RP, Bajpai VK. 1982. Oviduct acid mucus glycoproteins in the estrous rabbit: ultrastructure and histochemistry. Biol Reprod 26:155–168.
Killian G. 2011. Evidence that oviduct secretions influence sperm function: a retrospective view for livestock. J Anim Sci 89:1315–1322.
Kölle S, Dubielzig S, Reese S, Wehrend A, König P, Kummer W. 2009. Ciliary transport, gamete interaction, and effects of the early embryo in the oviduct: ex vivo analyses using a new digital videomicroscopic system in the cow. Biol Reprod 81:267–274.
Lantz KC, Enders AC, Liu IK. 1998. Possible significance of cells within intraluminal collagen masses in equine oviducts. Anat Rec 252:568–579.
Leese HJ. 1983. Studies on the movement of glucose, pyruvate and lactate into the ampulla and isthmus of the rabbit oviduct. Quart J Exp Physiol 68:89–96.
Leese HJ, Tay JR, Sandra J. 2001. Formation of fallopian tubal fluid: role of a neglected epithelium. Downing Reproduction 121: 339–346.
Lewis AW, Berardinelli JG. 2001. Gross anatomical and histomorphometric characteristics of the oviduct and uterus during the pubertal transition in sheep. J Anim Sci 79:167–175.
Muglia U, Motta PM. 2001. A new morpho-functional classification of the Fallopian tube based on its three-dimensional myoarchitecture. Histol Histopathol 16:227–237.
Nayak RK, Ellington EF. 1997. Ultrastructural and ultracytochemical cyclic changes in the bovine uterine tube (oviduct) epithelium. Am J Vet Res 38:157–168.
Nelis HM, Goossens K, Leemans B, Peelman L, and Van Soom A. 2012. Steroid-regulated mRNA expression in oviduct epithelial cells in the mare. Reprod Fertil Dev 25(1), Abstract 220.
Nieder GL, Macon GR. 1987. Uterine and oviducal protein secretion during early pregnancy in the mouse. J Reprod Fertil 81:287–294.
Oliphant G. 1986. Biochemistry and immunology of oviductal fluid. In: Siegler AM, editor. The fallopian tube: basic studies and clinical contributions. Mount Kisco, New York: Futura. p 129–145.
Orihuela PA, Ortiz ME, Croxatto HB. 1999. Sperm migration into and through the oviduct following artificial insemination at different stages of the estrous cycle in the rat. Biol Reprod 60:908–913.
Pedrero-Badillo F, Anaya-Hernández A, Corona-Quintanilla DL, Castelán F, Pacheco P, Martínez-Gómez M, Cuevas E. 2013.

Morphohistological characteristics of rabbit oviduct: a proposal for a single regionalization. Anim Reprod Sci 143:102–111.

Rigby JP. 1968. The length of the uterine horn and fallopian tube. Res Vet Sci 9:551–556.

Sostaric E, Dieleman SJ, van de Lest CH, Colenbrander B, Vos PL, Garcia-Gil N, Gadella BM. 2008. Sperm binding properties and secretory activity of the bovine oviduct immediately before and after ovulation. Mol Reprod Dev 75:60–74.

Steinhauer N, Boos A, Günzel-Apel AR. 2004. Morphological changes and proliferative activity in the oviductal epithelium during hormonally defined stages of the oestrous cycle in the bitch. Reprod Dom Anim 39:110–119.

Suárez SS. 2002. Formation of a reservoir of sperm in the oviduct. Reprod Dom Anim 37:140–143.

Suárez SS. 2008. Regulation of sperm storage and movement in the mammalian oviduct. Int J Dev Biol 52:455–462.

Suárez SS, Brockman K, Lefebvre R. 1997. Distribution of mucus and sperm in bovine oviduct after artificial insemination: the physical environment of the oviductal sperm reservoir. Biol Reprod 56:447–453.

Suárez SS, Refern K, Raynor P, Martin F, Phillips DM. 1991. Attachment of boar sperm to mucosal explants of oviduct in vitro: possible role in formation of a sperm reservoir. Biol Reprod 44: 998–1004.

Suzuki H and Tsutsumi Y. 1979. Morphological studies on the oviductal mucosa of the mare. J Fac Agr Hokkaido Univ 59(3):267–277.

Teilmann SC, Clement CA, Thorup J, Byskov AG, Christensen ST. 2006. Expression and localization of the progesterone receptor in mouse and human reproductive organs. J Endocrin 191: 525–535.

Thomas PGA, Ball BA, Brinsko SP. 1994. Interaction of equine spermatozoa with oviduct epithelial cell explants is affected by estrous cycle and anatomic origin of explant. Biol Reprod 51:222–228.

Trautman A and Fiebiger J. 1952. Fundamentals of the Histology of Domestic Animals. Ithaca, New York: Comstock Pub Assoc.

Tummaruk P, Tienthai P. 2010. Number of spermatozoa in the crypts of the sperm reservoir at about 24h after a low-dose intrauterine and deep intrauterine insemination in sows. Reprod Dom Anim 45:208–213.

Verhage HG, Fazleabas AT. 1988. The in vitro synthesis of estrogen-dependent proteins by the baboon *(Papio anibis)* oviduct. Endocrinology 123:522–558.

Weber JA, Freeman DA, Vanderwall DK, Woods GL. 1991. Prostaglandin E2 secretion by oviductal transport-stage equine embryos. Biol Reprod 45:540–543.

Willis P, Sekhar KNC, Brooks P, Fayrer-Hosken RA. 1994. Electrophoretic characterization of equine oviductal fluid. J Exp Zool 268:477–485.

Wrobel KH, Kujat R, Fehle G. 1993. The bovine tubouterine junction: general organization and surface morphology. Cell Tissue Res 271:227–239.

Wu ASH, Carlson SD, First NL. 1976. Scanning electron microscopic study of the porcine oviduct and uterus. J Anim Sci 42:804–809.

Yániz JL, Carretero T, Recreo P, Arceiz E, Santolaria P. 2013. Three-dimensional architecture of the ovine oviductal mucosa. Anat Histol Embryol 38:1–10.

Yániz JL, Lopez-Gatius F, Hunter RH. 2006. Scanning electron microscopic study of the functional anatomy of the porcine oviductal mucosa. Anat Histol Embryol 35:28–34.

Yániz JL, Lopez-Gatius F, Santolaria P, Mullins JK. 2000. Study of the functional anatomy of bovine oviductal mucosa. Anat Rec 260: 268–278.